Doped TiO$_2$ Photocatalysts for the Photocatalytic Degradation Efficiency of Methylene Blue and Humic Acid under Solar Light

Nazli Turkten[1] and **Miray Bekbolet**[2]
[1]Kirsehir Ahi Evran University, Department of Chemistry, Kirsehir, Turkey
[2]Bogazici University, Institute of Environmental Sciences, Istanbul, Turkey

ABSTRACT

In various advanced oxidation processes, photocatalysis is a promising and efficient way? to remove natural organic matter consisting of humic acids and fulvic acids. The principle of this method involves both usage of a semiconductor photocatalyst and O$_2$ for the generation of radicals. Among them, TiO$_2$ photocatalysis is the most popular and studied one since TiO$_2$ has unique properties such as being chemically inert, photocatalytically stable, cheap, non-toxic, environmentally benign and exhibiting high oxidative power. However, despite all the advantages of using TiO$_2$ as a photocatalyst, there is a major disadvantage. Since TiO$_2$ has a broad band gap, its usage widely under solar light is limited and only allows to be active under UV light. Doping is one of the most popular methods to enhance the photocatalytic activity of TiO$_2$ via using metal or non-metal species as dopants. In this respect, solar light sensitive TiO$_2$ photocatalyst, C, N, S, Se doped and S/N codoped TiO$_2$ photocatalysts were synthesized by using wet-impregnation method. These doped photocatalysts were characterized by Raman spectroscopy to determine the crystal surface morphology. Moreover, methylene blue was used to investigate the photocatalytic performance of prepared doped TiO$_2$ photocatalysts in the presence or absence of organic matrix. Photocatalytic experiments were performed using a solar light simulating photoreactor. Humic acid characterization was monitored by UV-vis and fluorescence spectroscopy.

Keywords:
Raman spectroscopy; Metal/non-metal doped TiO$_2$; Humic acid; Photocatalysis.

INTRODUCTION

Wastewater is polluted with severe concentration of dyes in industries such as textile, cosmetic, paper, leather, food, etc. and this causes a critical environmental and health public issue [1, 2]. Accordingly, many studies have been reported for the removal of these colored effluents from wastewater using different methods such as physicochemical treatments, chemical methods, advanced oxidation processes (AOPs), and biological methods [3-8]. The application of the physicochemical treatments are limited because of the formation of sludge to be disposed of or the need of regeneration of the adsorbent materials. Although, biological methods are environmentally friendly and inexpensive, they are not effective to degrade the dyes in wastewaters and thus uncompleted degradation can cause secondary pollution. Even if ozonation is an effective process for the decolorization of dyes, this method causes very high operating costs [2, 9-11].

Among AOPs, heterogeneous photocatalysis in which a semiconductor, such as TiO$_2$, ZnO, SnO$_2$, etc. is used as a photocatalyst is an effective alternative method to conventional methods. TiO$_2$ photocatalysis is based on the formation of photogenerated charge carriers on the surface of titanium dioxide. Photocatalytic mechanism is initiated with the excitation and transfer of an electron from the valence band to the conduction band of TiO$_2$ and positively charged holes are formed in the valence band at the same time. These generated electron-hole reacts with water and O$_2$ or OH$^-$ to form extremely reactive oxygen species (ROS) such as superoxide anions, and hydroxyl radicals. During the photocatalytic process, hydroxyl radicals react with surface adsorbed pollutants and leads them to degrade. Subsequently, further reactions with ROS could mineralize the organic matter to carbon dioxide and water [3, 4, 12].

TiO$_2$ is the most popular and promising photocatalyst with great photosensitivity and chemical stability. Moreover, it is non-toxic and a low-cost material. Nevertheless, TiO$_2$ with wide and gap of E$_{bg}$=3.2 eV limits its photocatalytic activity under solar light (This sentence needs correcting). Thus, doping method by using metal ions i.e. Cu, V, Se, Fe, etc., non-metal elements i.e. B, C, S, N, etc. and co-doping with metals and non-metals (N/S, N/Se, etc.) has been used to improve the photocatalytic activity of TiO$_2$ as an effective strategy under visible light [5, 7, 12-18].

In this study, C, N, S, Se doped and N/S codoped TiO$_2$ photocatalysts were synthesized by wet-impregnation method. Crystal surface morphology of the doped TiO$_2$ photocatalyts was determined by using Raman Spectroscopy. Photocatalytic acitivity of these specimens were investigated using methylene blue (MB) as a basic dye under simulated solar light in presence and absence of humic acid (HA).

MATERIAL AND METHODS

Materials

Commercial HA (humic acid sodium salt) was purchased from Aldrich. TiO$_2$ Evonik P25 was used as the photocatalyst for doping procedure. Doped TiO$_2$ photocatalysts were synthesized via an incipient wet-impregnation method using C$_6$H$_{12}$O$_6$ (glucose), CH$_4$N$_2$O (urea), NH$_2$CSNH$_2$ (thiourea), SeCl$_4$ (selenium tetrachloride) and CH$_4$N$_2$O coupled with NH$_2$CSNH$_2$ (urea and thiourea) as C, N, S, Se and S/N sources, respectively. All doping sources and MB were purchased from Merck. Distilled water was used for the preparation of the solutions. The chemical structures of MB and HA are given in Fig. 1.

Preparation of Doped TiO$_2$ Photocatalysts

Dopant concentration was selected as 0.50% wt. for all photocatalysts as it was determined in previous work [13-

18]. In incipient wet-impregnation method, 0.50% dopant agents in 15 mL water was added to 10 g TiO2 Evonik P25 and stirred for 1 h at room temperature. Afterwards, doped photocatalysts were washed with distilled water, dried in air oven at 378 K for 24 h, and calcined at a predetermined temperature and time which were given in Table 1. Finally, the obtained samples were ground and passes through a sieve (32 Micron) to achieve a more homogeneous size distribution.

Table 1. Calcination time and temperature for the prepared photocatalysts.

	Photocatalyst	Synonym	Temperature & Calcination
1	C-doped TiO$_2$	C-350-3-TiO$_2$	350°C 3h
		C-500-3-TiO$_2$	500°C 3h
2	N-doped TiO$_2$	N-350-3-TiO$_2$	350°C 3h
		N-500-3-TiO$_2$	500°C 3h
3	S-doped TiO$_2$	S-350-3-TiO$_2$	350°C 3h
		S-500-3-TiO$_2$	500°C 3h
4	Se-doped TiO$_2$	Se-350-3-TiO$_2$	350°C 3h
5	N/S-codoped TiO$_2$	N/S-350-3-TiO$_2$	350°C 3h

Solar Photocatalytic Experiments

Atlas-Suntest CPS+ solar simulator was used for the photocatalytic experiments [16]. The solar degradation of MB (20 mg/L) using doped TiO$_2$ specimens under solar light with 60 min irradiation time in presence and absence of HA (20 mg/L) was investigated. After the photocatalytic process, TiO$_2$ was removed by a filtration process. The photocatalytic experiments were carried out without pH adjustment (pH~5.5).

Characterization

Absorbance of filtered MB solutions at λ=662 nm was monitored by UV-vis spectrophotometry (Perkin Elmer lambda 35). EEM fluorescence spectra was measured by a Luminescence Spectrometer (Perkin Elmer LS 55). The detailed procedure was given in our previous work [16]. Raman spectra were acquired by a Thermo Scientific NXR FT-Raman spectrometer using Ar$^+$ laser excitation at λ=532 nm, with a laser power 10 mW and a resolution 2 cm^{-1}.

RESULTS AND DISCUSSION

Raman Spectroscopy

Raman spectroscopy was employed for the characterization of the surface structure and identifying the phase transformation of doped TiO^2 photocatalysts. Moreover,
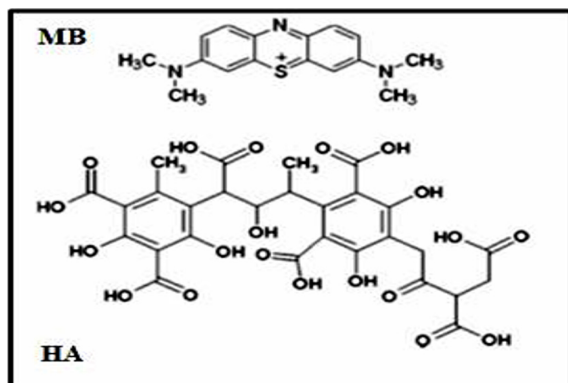

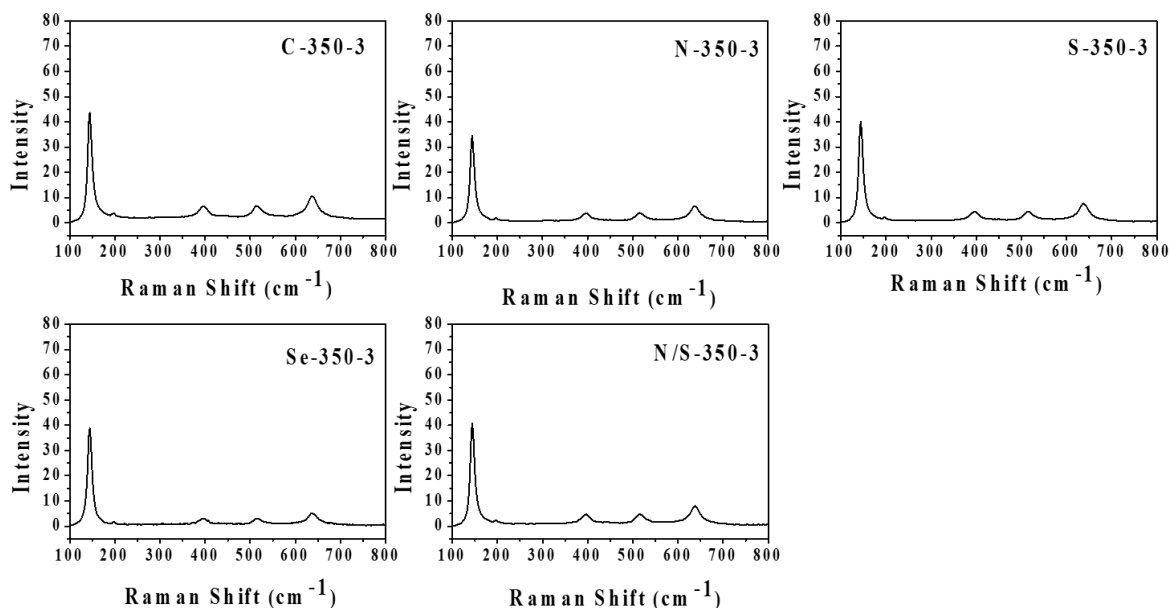**Figure 1.** Chemical structures of MB and Steelink's proposed unit structure of HA [19].

Figure 2. FT-Raman spectra of doped TiO$_2$ samples calcined at 350°C for 3h.

the effect of different dopant agents and different calcination temperatures on the transformation of crystallographic phases were identified. The FT-Raman spectra of the doped TiO$_2$ samples calcined at 350°C for 3h are displayed in Fig. 2.

Raman peaks were acquired at 144 (E$_g$), 197 (E$_g$), 397 (B$_{1g}$), 515 (A$_{1g}$, B$_{1g}$), and 637 (E$_g$) cm^{-1} in the spectra of each sample, indicating the presence of anatase phase [16, 20]. Similarly, Raman spectroscopy of the samples calcined at 500°C for 3h (Fig. 3) revealed the presence of only anatase phase.

Any phase transformation from anatase phase to rutile phase and any significant shift in the Raman bands were not observed as expected. The reason could be explained by the anatase phase transformation to rutile phase starting at 550°C [21].

Photocatalytic Experiments

Photocatalyst performances were estimated by the removal percentage values of MB in the absence and presence of HA. Removal percentages were determined from Equation (1), where C$_0$ is the initial concentration of MB and C is concentration at time t of MB.

$$\mathrm{Re}\,moval\% = \frac{C_0 - C}{C_0} x100 \qquad (1)$$

In Fig. 4 (a), removal % values of MB by using doped TiO$_2$ photocatalysts under solar light at 60 min are shown. Se-350-3 and N-350-3 TiO$_2$ photocatalysts exhibited the

highest removal of MB as 87.30% and 89.31%, respectively. It was found that N/S-350-3 TiO$_2$ has the lowest ability for the decolorization of MB compared to other doped photocatalysts. Moreover, the effect of calcination temperature on the anion doped photocatalysts (C-doped TiO$_2$, N-doped TiO$_2$ and S-doped TiO$_2$ photocatalysts) were investigated and shown in Fig. 4 (b). N-doped and C-doped TiO$_2$ photocatalysts almost exhibited the same removal efficiency, while S-doped TiO$_2$ samples performed a lowered photocatalytic activity with increasing calcination temperature. The reason may be explained by its having a large surface area compared to N-doped and C-doped TiO$_2$ samples which were reported in our previous work [13]. A larger surface area could promote an increment on the photogenerated electrons and photocatalytic activity [22]. For this reason, a further study is needed to investigate the removal percentage of anionic dyes by using anion doped TiO$_2$ photocatalysts.

In Fig. 4 (c), the removal % efficiency of MB with the presence of HA is shown. HA caused a retardation effect on the photocatalytic system. The reason of this retardation could be explained by two assumptions.

i)HA could reduce the light transmittance thereby effects photo-oxidation process.

ii) The competition between HA and MB for the active sites of TiO$_2$ surface [23].

Fig. 5 displays the UV-vis spectra of MB solution with the absence and presence of HA after 60 min for doped TiO$_2$ photocatalysts. The spectrum of MB was characte-
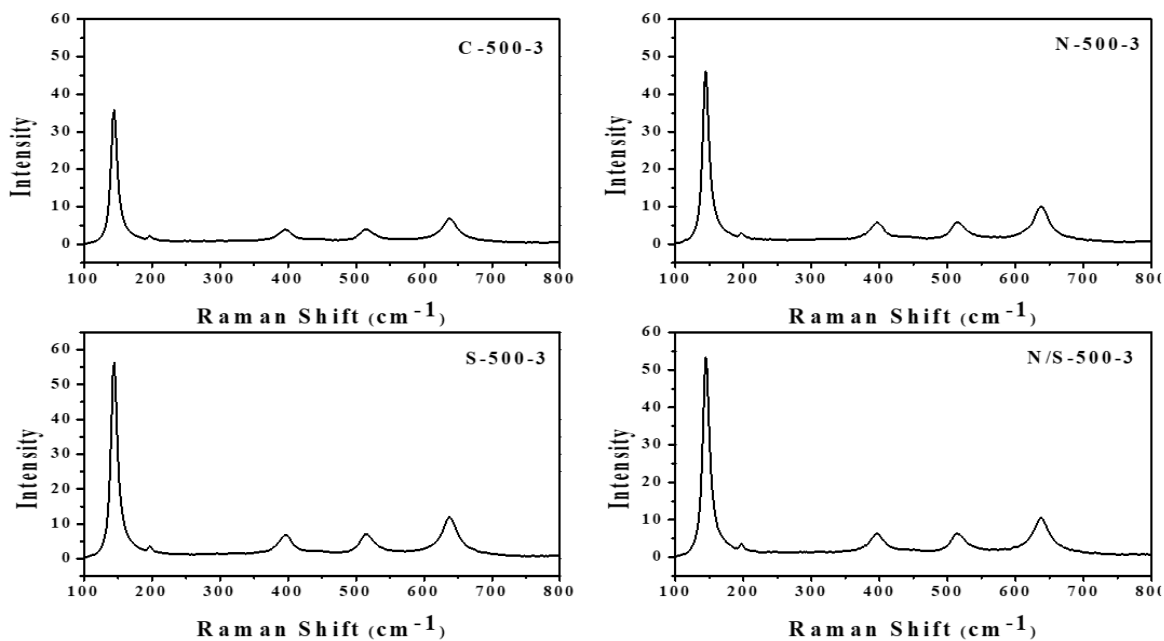
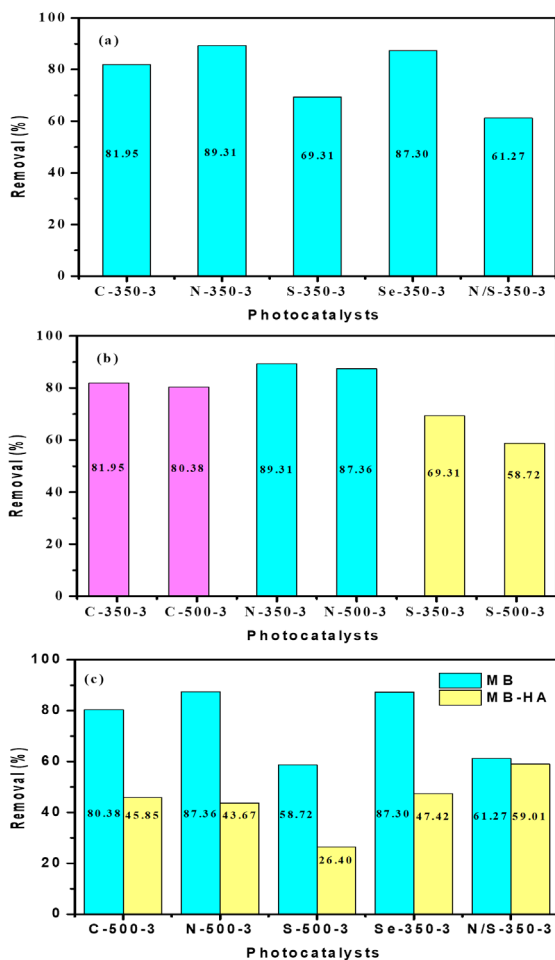**Figure 3.** FT-Raman spectra of doped TiO$_2$ samples calcined at 500°C for 3 h.

Figure 4. The removal % values of MB **(a)** 350°C 3h, **(b)** 350°C and 500°C 3h, **(c)** the retardation effect of HA.

rized by an absorption band λ=662 nm and a shoulder at 612 nm in visible light region. This absorption band was attributed to a chromophore including an elongated conjugate system. The absorption bands located in the UV region at 292 nm and 245 nm were corresponded to the conjugated system of the benzene ring structure [24, 25].

In Fig. 5 (a) and (b), the characteristic absorption peak of MB solution at 662 nm was significantly lowered in intensity with solar light irradiation and the shoulder was disappeared. Furthermore, a decrease in the intensity of benzene rings after irradiation, confirmed that decolorization and degradation of MB occurs at the same time. Among all doped TiO$_2$ photocatalysts, N-TiO$_2$ was the most effective one and decolorize approximately 87-89% of MB after 60 min. In Fig. 5 (c), the presence of HA effected the disappearance of hump at 612 nm after irradiation. Besides, the intensity of aromatic peaks and maximum absorption peak were decreased as expected after 60 min. However, the retardation effect of HA caused an adverse impact by decreasing the intensity of peaks compared to the peaks in absence of HA spectra.

EEM Fluorescence Contour Plots

Regional specification of the EEM spectra of HA was expressed in four regions. Region I, II and III were defined as aromatic proteins I, aromatic proteins II and fulvic-like in the excitation wavelength region of λ$_{exc}$=200−250 nm with emission wavelength regions of λ$_{emis}$=280−332 nm, λ$_{emis}$=332−380 nm and λ$_{emis}$=380−580 nm respectively.
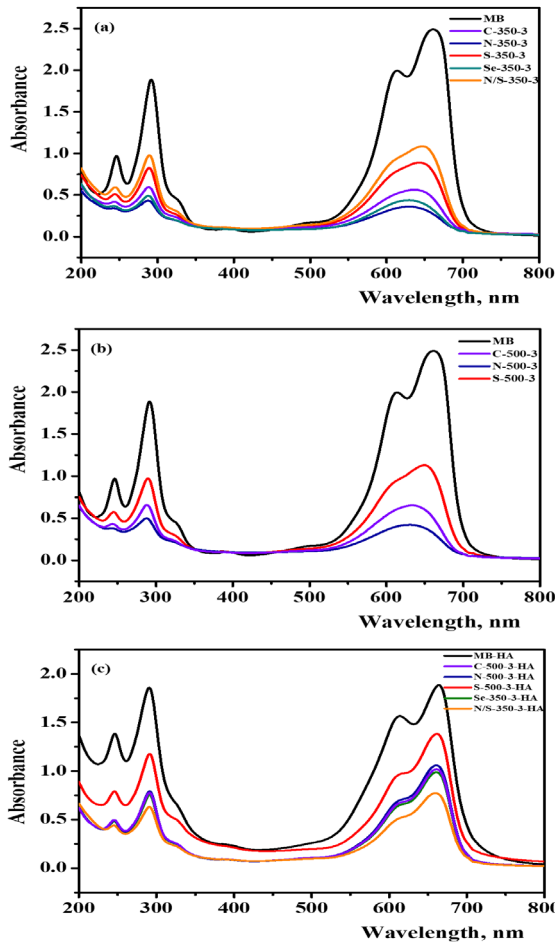
Figure 5. UV-vis spectra of MB dye solution by doped TiO$_2$ photocatalysts **(a)** 350°C 3h, **(b)** 350°C and 500°C h, **(c)** presence of HA.

Region IV and V were expressed by microbial byproducts and humic-like in the excitation wavelength region of λ_{exc}=250−470 nm with an emission wavelength region of λ_{emis}=280−380 nm and λ_{emis}=380−580 nm respectively [26].

In Fig. 6, EEM contour plots of HA and MB subsequent to photocatalysis of 60 min using doped-TiO$_2$ samples are shown. It is notable from the figure that humic-like features decreased in all spectra after 60 min irradiation, but the most significant changes were observed in the presence of N-TiO$_2$, C-TiO$_2$, and Se-TiO samples. The humic-like region was slightly decreased in S-TiO$_2$ and N/S-TiO$_2$ samples compared to anion doped TiO$_2$ samples.

CONCLUSION

In this study, C, N, S, Se doped and N/S codoped TiO$_2$ photocatalysts were prepared using wet-impregnation method. It was found that Se-350-3 and N-350-3 TiO$_2$ photocatalysts exhibited the highest removal of MB. The removal efficiency % was decreased in HA medium because of the retardation effect of HA on the photocatalytic system. In Raman spectra, any phase transformation from anatase phase to rutile phase was not observed due to different calcination temperature as expected. The results in Raman spectra confirmed that all doped TiO$_2$ photocatalysts exhibited anatase phase. In accordance with removal data, the change of EEM spectra with a decrease in intensity of the humic-like region was noticable after 60 min irradiation especially in anion doped TiO$_2$ photocatalysts.
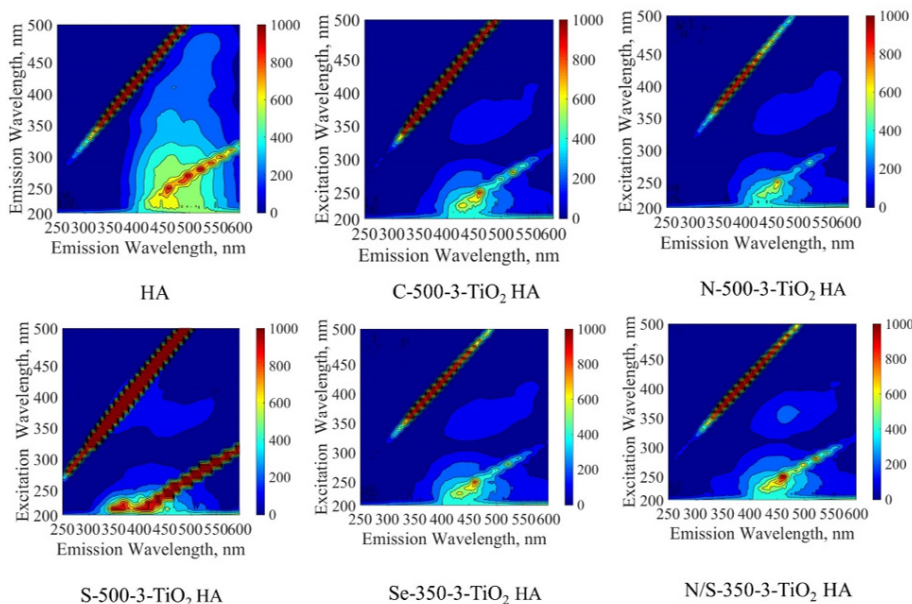

Figure 6. EEM contour plots of HA and MB with respect to irradiation 60 min using doped TiO$_2$.

ACKNOWLEDGEMENT

References

1. Aksakal O., Ucun H.. Equilibrium, kinetic and thermodynamic studies f the biosorption of textile dye (Reactive Red 195) onto Pinus sylvestris L.Journal of Hazardous Materials 181 (2010) 666-672.

2. Brillas E., Martínez-Huitle C.A. Decontamination of wastewaters containing synthetic organic dyes by electrochemical methods. An updated review, Applied Catalysis B: Environmental 166-167 (2015) 603-643.

3. Bora L.V., Mewada R.K. Visible/solar light active photocatalysts for organic effluent treatment: Fundamentals, mechanisms and parametric review, Renewable and Sustainable Energy Reviews 76 (2017) 1393-1421.

4. Byrne C., Subramanian G., Pillai S.C. Recent advances in photocatalysis for, environmental applications, Journal of Environmental Chemical Engineering 6 (2018) 3531-3555.

5. Pelaez M., Nolan N.T., Pillai S.C., Seery M.K., Falaras P., Kontos A.G., Dunlop P.S.M., Hamilton J.W.J., Byrne J.A., O'Shea K., Entezari M.H., Dionysiou D.D. A review on the visible light active titanium dioxide photocatalysts for environmental applications Applied Catalysis B: Environmental, 125 (2012) 331-349.

6. Srikanth B., Goutham R., Badri Narayan R., Ramprasath A., Gopinath K.P., Sankaranarayanan A.R. Recent advancements in supporting materials for immobilised photocatalytic applications in waste water treatment, Journal of Environmental Management, 200 (2017) 60-78.

7. Zangeneh H., Zinatizadeh A.A.L., Habibi M., Akia M., Hasnain Isa M. Photocatalytic oxidation of organic dyes and pollutants in wastewater using different modified titanium dioxides: A comparative review, Journal of Industrial and Engineering Chemistry, 26 (2015) 1-36.

8. Uyguner-Demirel C.S., Birben C.N., Bekbolet M. A comprehensive review on the use of second generation TiO2 photocatalysts: Microorganism inactivation, Chemosphere, 211 (2018) 420-448.

9. Farabegoli G., Chiavola A., Rolle E., Naso M. Decolorization of Reactive Red 195 by a mixed culture in an alternating anaerobic–aerobic Sequencing Batch Reactor, Biochemical Engineering Journal 52 (2010) 220-226.

10. Forgacs E., Cserháti T., Oros G. Removal of synthetic dyes from wastewaters: a review, Environment International 30 (2004) 953-971.

11. Martínez-Huitle C.A., Brillas E. Decontamination of wastewaters containing synthetic organic dyes by electrochemical methods: A general review, Applied Catalysis B:Environmental 87 (2009) 105-145.

12. Khaki M.R.D., Shafeeyan M.S., Raman A.A.A., Daud W.M.A.W. Application of doped photocatalysts for organic pollutant degradation - A review, Journal of Environmental Management 198 (2017) 78-94.

13. Birben N.C., Uyguner-Demirel C.S., Sen-Kavurmaci S., Gürkan Yelda Y., Türkten N., Kılıç M., Çınar Z., Bekbolet M. Photocatalytic Performance of Anion Doped TiO2 on the Degradation of Complex Organic Matrix, in:Journal of Advanced Oxidation Technologies 2016, pp. 199.

14. Birben N.C., Uyguner-Demirel C.S., Kavurmaci S.S., Gürkan Y.Y., Turkten N., Cinar Z., Bekbolet M. Application of Fe-doped TiO$_2$ specimens for the solar photocatalytic degradation of humic acid Catalysis Today, 281 (2017) 78-84.

15. Birben N.C., Uyguner-Demirel C.S., Sen-Kavurmaci S., Gurkan Y.Y., Turkten N., Cinar Z., Bekbolet M. Comparative evaluation of anion doped photocatalysts on the mineralization and decolorization of natural organic matter Catalysis Today, 240, Part A (2015) 125-131.

16. Turkten N., Cinar Z., Tomruk A., Bekbolet M., Copper-doped TiO$_2$ photocatalysts: application to drinking water by humic matter degradation, Environmental science and pollution research international, 36 (2019) 36096–36106.

17. Gurkan Y., Kasapbasi E., Turkten N., Cinar Z. Influence of Se/N codoping on the structural, optical, electronic and photocatalytic properties of TiO$_2$ Molecules, 22 (2017) 414.

18. Birben N.C., Tomruk A., Bekbolet M. The role of visible light active TiO$_2$ pecimens on the solar photocatalytic disinfection of E. coli, Environmental science and pollution research international, 24 (2017) 12618-12627.

19. Tan K.H. Humic Matter in soil and the environment: principles and controversies, Second Edition, CRC PressTaylor & Francis Group 6000, Broken Sound Parkway NW, Suite 300Boca Raton, FL, pp. 240.

20. Bassi A.L., Cattaneo D., Russo V., Bottani C.E., Barborini E., Mazza T., Piseri P., Milani P., Ernst F.O., Wegner K., Pratsinis S.E. Raman spectroscopy characterization of titania nanoparticles produced by flame pyrolysis: The influence of size and stoichiometry Journal of Applied Physics, 98 (2005) 074305.

21. Mathpal M.C., Tripathi A.K., Singh M.K., Gairola S.P., Pandey S.N., Agarwal A., Effect of annealing temperature on Raman spectra of TiO2 nanoparticles, Chemical Physics Letters, 555 (2013) 182-186.

22. Tian H., Ma J., Li K., Li J. Hydrothermal synthesis of S-doped TiO$_2$ nanoparticles and their photocatalytic ability for degradation of methyl, orange, Ceramics International 35 (2009) 1289-1292.

23. Lin C., Lin K.S. Photocatalytic oxidation of toxic organohalides with TiO2/UV: the effects of humic substances and organic mixtures Chemosphere, 66 (2007) 1872-1877.

24. Liu X., Yang Y., Shi X., Li K. Fast photocatalytic degradation of methylene blue dye using a low-power diode laser, Journal of Hazardous Material, 283 (2015) 267-275.

25. Yu X., Huang L., Wei Y., Zhang J., Zhao Z., Dai W., Yao B. Controllable preparation, characterization and performance of Cu$_2$O thin film and photocatalytic degradation of methylene blue using response surface methodology, Materials Research Bulletin 64 (2015) 410-417.

26. Sen-Kavurmaci S., Bekbolet M. Tracing TiO$_2$ photocatalytic degradation of humic acid in the presence of clay particles by excitation–emission matrix (EEM) fluorescence spectra, Journal of Photochemistry and Photobiology A:Chemistry, 282 (2014) 53-61.